Effect of Aging and Ice Structuring Proteins on the Morphology of Frozen Hydrated Gluten Networks

Vassilis Kontogiorgos and H. Douglas Goff*

Department of Food Science, University of Guelph, Guelph, Ontario, Canada N1G2W1

Stefan Kasapis

Department of Chemistry, National University of Singapore, Block S3, Level 6, Science Drive 4, Singapore 117543

Received November 1, 2006; Revised Manuscript Received January 25, 2007

The present investigation constitutes an attempt to rationalize the effect of aging and ice structuring proteins (ISPs) on the network morphology of frozen hydrated gluten. In doing so, it employs differential scanning calorimetry, time-domain NMR, dynamic oscillation on shear, creep testing, and electron microscopy. Experimentation and first principles modeling allows identification and description of the processes of ice formation and recrystallization in molecular terms. It is demonstrated that in the absence of a readily discernible glass transition temperature in gluten−ice composites, the approach of considering the melting point and aging at constant or fluctuating temperature conditions in the vicinity of this point can provide a valid index of functional quality. A theoretical framework supporting the concept of capillary confined frozen water in the gluten matrix was advanced, and it was found that ISPs were effective in controlling recrystallization both within these confines and within ice in the bulk.

Introduction

Wheat storage proteins are mainly comprised of gliadins and glutenins. Gliadins are present as monomers with M_w ranging from 3 to 8 × 10^4 Da, whereas the glutenin fraction is comprised of aggregated proteins in which individual polypeptides are thought to be linked via interchain disulfide bonds to give a wide M_w distribution that ranges between 10^5 and 10^7 Da.[1,2] Upon hydration, gluten proteins form a three-dimensional network, and several concepts have been put forward to describe the morphology of the network, such as the loop and train,[3] the entanglement,[4] or the particulate network model.[5,6] Theoretical rationalizations of mechanical functions are supported by empirical data on the thermal (DSC) properties and water mobility, thus guiding technological features and applications of the material.

Subzero temperatures result in dramatic changes in the physicochemical properties of the hydrated gluten network owing to ice formation and isothermal or temperature fluctuation driven ice recrystallization. Partial loss of network functionality and water holding capacity has been documented using, for example, microscopy and thermomechanical analysis for materials obtained from various sources.[7−10] It follows that incorporation in the matrix of a functional agent to regulate these outcomes is an attractive proposition. Antifreeze proteins (AFPs), also known as ice structuring proteins (ISPs),[11] may possess such a property. ISPs are synthesized by various organisms (fish, plants, or insects) so that their cells survive subzero environmental surroundings and exhibit some or all of the three main properties of non-colligative freezing point depression (thermal hysteresis), ice nucleation, and recrystallization inhibition.[12,13]

* Corresponding author. E-mail: dgoff@uoguelph.ca; tel.: + 519 824 4120, ext. 53878; fax: + 519 824 6631.

Table 1. TD-NMR Experimental Settings

90° (μs)	180° (μs)	no. of scans	recycle delay (s)	gain	τ (ms)	detection mode
3.88	8.02	8	2	64	0.5	magnitude

The generally accepted mechanism of ice growth inhibition is based on the Kelvin effect.[14−16] According to this school of thought, the protein acts as a structural impurity, and upon adsorption onto the crystal, a curved surface is formed. The solubility of this interface is increased with a decreasing radius of curvature. Further ice crystal formation at isothermal conditions is increasingly difficult owing to the irregularity and instability/solubility of the supercooled water−protein interface. In this respect, studies of the biochemical and physical properties of cold-acclimated winter wheat grass extracts suggest that preparations are able to retain recrystallization inhibition activity even after they are subjected to an extensive heat treatment.[17,18]

ISPs from the aforementioned source with recrystallization inhibition activity were identified to be thaumatin-like in nature (i.e., a polypeptide of about 21 kDa with a β-sheet and random coil solution conformation).[18] It appears that the binary mixture of an ice structuring protein and gluten is suitable for fundamental work on the physicochemical properties of the latter in the form of a frozen polymeric matrix, which possesses considerable technological interest. The objective of the present investigation, therefore, is to carry out such a study by varying the subzero thermal regime of the mixture and examining the effect of aging and ice structuring proteins on the network morphology of hydrated gluten.

Experimental Procedures

Materials and Sample Preparation. Gluten was purchased from Sigma-Aldrich (St. Louis, MO). The raw cold-acclimated winter wheat

10.1021/bm0610471 CCC: $37.00
Published on Web 03/07/2007

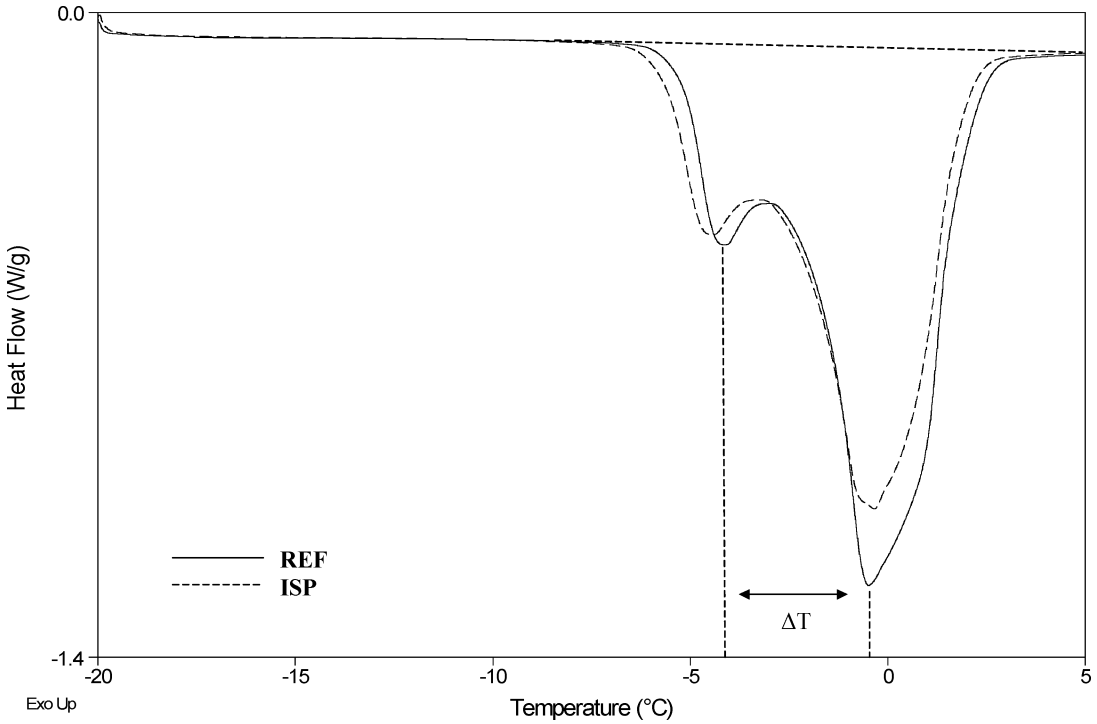

Figure 1. DSC thermograms of frozen hydrated gluten (40% w/w) following 30 days of aging at fluctuating temperature conditions. ISP and REF are the samples with (0.1% w/v) and without ice structuring proteins, respectively (heating rate is 1 °C/min).

Table 2. Enthalpy of Ice Melting and Pore Radius Sizes of Frozen Hydrated Gluten (40% w/w)

	enthalpy of melting (J/g)				pore radius (nm)			
time (days)	REF_{const}	ISP_{const}	REF_{fluc}	ISP_{fluc}	REF_{const}	ISP_{const}	REF_{fluc}	ISP_{fluc}
1	251.2^{ns}[a]	242.6^{ns}	255.5^{ns}	254.8^{ns}	4.3^{ns}	4.4^{ns}	3.9^{ns}	4.0^{ns}
10	259.7^{ns}	250.9^{ns}	266.5^{ns}	257.1^{ns}	5.2^{ns}	5.0^{ns}	4.1^{ns}	4.0^{ns}
20	259.1^{ns}	254.7^{ns}	271.4^{ns}	263.7^{ns}	5.7**	5.1**	5.2^{ns}	5.0^{ns}
30	272.3**[b]	248.2**	258.2^{ns}	252.9^{ns}	6.4**	5.5**	5.3^{ns}	5.1^{ns}

[a] ns: Difference between comparisons on the same day is not significant at $p > 0.05$. [b] **: Difference between comparisons on the same day is significant at $p < 0.01$.

(*Triticum aestivum*) grass extract was provided by Ice Biotech Inc. (Flamborough, ON, Canada). A highly active ISP preparation was isolated from the raw extract according to a procedure recently described in the literature.[18] Aqueous preparations were made in ultrapure water (Milli-Q) at a near neutral pH, and sodium azide (0.02% w/w) was added as a preservative. The ISP concentration in the stock solution of the present investigation was 33.5 mg/mL, and aliquots were removed to add to hydrated gluten described next.

Samples of hydrated gluten (40% w/w gluten solids, i.e., 60% w/w water for all samples irrespective of the experimental method) with 0.1% w/v ISP solids, or without ISP, were prepared, kneaded manually with a spatula, and left to hydrate at 4 °C for 30 min. Following equilibration, materials were stored either under constant or under fluctuating temperature conditions. In the former, storage at −13 ± 1 °C for 30 days was the experimental setting, whereas for the latter, temperatures of a chest freezer were programmed to vary, as follows: −20 °C for 12 h, heating to −10 °C at a rate of 0.8 °C/h, holding there for 12 h, and finally cooling once more to −20 °C at a rate of 0.8 °C/h. The thermal regime was run continuously for 30 days, and irrespective of the type of experimentation, samples were examined upon preparation (time 0) and after 1, 10, 20, and 30 days of aging.

Hereafter, the reference samples (i.e., without ISP) will be denoted as REF, while those containing ice structuring proteins will be referred to as ISP. Furthermore, samples stored under constant temperature conditions will be referred to as "const" in the subscript, and the said subscript will be replaced by "fluc" for those under a fluctuating storage temperature.

Differential Scanning Calorimetry. Samples of 15−25 mg were hermetically sealed in aluminum DSC pans (Alod-Al) and stored as described in the previous section. A sample handling technique was developed for their transfer from freezer to instrument to avoid ice melting that would negate the effect of aging or condensation on the surface of the pan. In doing so, a metallic container was used with two levels, and the bottom of the container (first level) was filled with liquid nitrogen. The second level, where the sample was placed, was made by a metallic mesh and stood 5 cm from the bottom so that the cold nitrogen vapors could saturate the environment surrounding the sample. Thus, the sample was held in a nitrogen atmosphere of about −30 °C during handling. The DSC cell was precooled at −20 °C, with the sample being equilibrated at that temperature for 5 min before scanning to 10 °C at a heating rate of 1 °C/min. We identified the sample transfer procedure as a critical step to obtain reproducible thermal traces.

T_{zero} calibration of the instrument (Q1000 MDSC, TA Instruments, New Castle, DE) was performed by heating the cells without pans in the temperature range of interest. Cell constant and temperature calibrations were performed with indium and MilliQ water, respectively, at a scan rate of 1 °C/min, and the heat capacity was calibrated using a sapphire standard. For all measurements, the reference was an empty pan, and the cell compartment was purged with nitrogen at a flow rate of 50 mL/min. Experiments were performed at least in triplicate, and averages of effectively overlapping traces are reported.

Time Domain-NMR Measurements. NMR probes (8 mm diameter) were filled approximately 6 cm from the bottom with sample, hermetically sealed with a lid, and stored as described previously. At the time of measurement, the samples were thawed for approximately

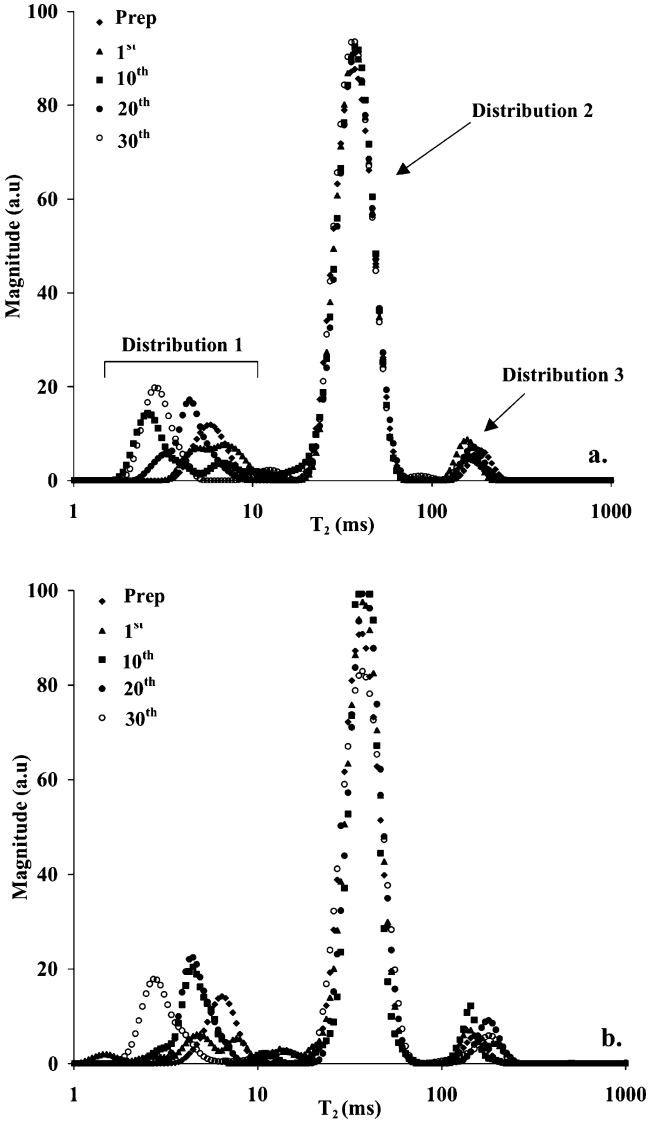

Figure 2. Typical T_2 relaxation distributions of hydrated gluten (40% w/w) aged at a constant temperature (−13 °C) for the number of days indicated (measurements were taken at 40 °C). (a) REF and (b) ISP.

8 h at room temperature and equilibrated at 40 °C, which was also the temperature of the magnet, in a circulating water bath. Following equilibration, the samples were subjected to T_2 relaxation measurements on a Bruker mq20 Series NMR Analyzer (Bruker, Milton, ON, Canada). A Carr−Purcell−Meiboom−Gill (CPMG) pulse sequence was used to determine the spin−spin relaxation times. Experimental settings that facilitate measurements are shown in Table 1. The operational pulse length was obtained using the calibration procedures recommended by the manufacturer on unfrozen samples (40 °C) analyzed on the day of preparation. This allowed determination of the Gain and Recycle Delay parameters in the course of a single pulse experiment (FID). Tau (τ) was selected to be as short as possible to minimize chemical exchange and diffusion effects on the decay curves. Three measurements were taken for each experimental treatment from two different batches yielding in total six replicates for each treatment.

Rheological Measurements. Samples were weighed (10 g), wrapped in a plastic membrane to minimize possible sublimation, and stored at constant or fluctuating temperature conditions as described previously. Samples were removed from the freezer and thawed at ambient temperature for approximately 8 h, and a portion of each was subjected to small deformation oscillatory measurements or creep testing using a controlled stress rheometer (AR-1000N, TA Instruments Ltd., Leatherhead, UK). Parallel plate geometry of 40 mm diameter and 2

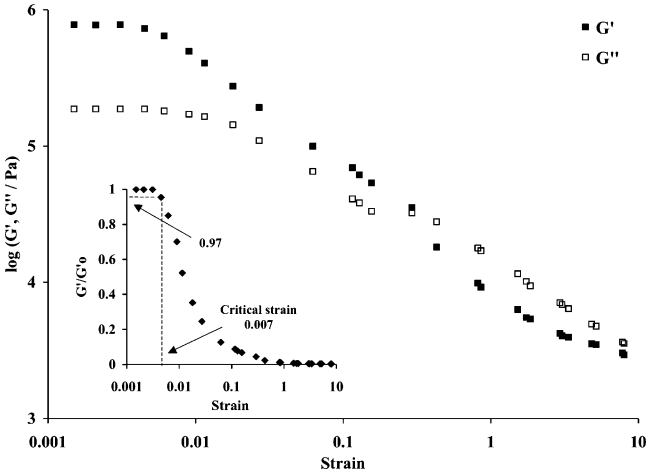

Figure 3. Strain sweep measurements of G' and G'' for hydrated gluten (40% w/w), with the inset pinpointing the limits of the linear viscoelastic region (frequency of 1 Hz).

mm gap was employed throughout. Excess material was trimmed off the edges of the plates, and materials were allowed to relax at 20 °C. It was ascertained that within 15 min of the time sweep carried out at 1 Hz (approximately 6.28 rad/s) and 0.005 strain (0.5%), the elastic (storage modulus; G') and viscous (loss modulus; G'') components of the network reached a pseudo-equilibrium plateau. Frequency sweeps were carried out at the same temperature and applied strain covering a range of 0.01−100 Hz. The experimental routine was completed with transient measurements. In doing so, the desired stress (80 Pa) was applied instantaneously to the sample, and the angular displacement was monitored for 20 min (retardation curve). A solvent trap was used to minimize moisture loss from the edges of the sample. Dynamic measurements were conducted in triplicate and creep measurements in duplicate. Nonlinear regression of the experimental data was performed using GraphPad Prism v. 4.00 (GraphPad Software, San Diego, CA).

Cryo-SEM Observations. Samples were weighed (10 g), wrapped in a plastic membrane, and stored at constant or fluctuating temperature conditions as described previously. After 1, 10, 20, or 30 days of aging, they were unwrapped and immersed immediately in liquid nitrogen, fractured (under liquid nitrogen), placed in a copper sample holder, and transferred to a cryo-preparation unit using a transfer device (Emscope SP2000A Sputter-cryo, Emscope Ltd., Kent, UK). Specimens were fractured once more with a blade in the preparation chamber to expose a fresh surface and sublimated at −80 °C for 30 min. Following sublimation, specimens were gold sputter-coated for 2 min and transferred to the cryo-SEM microscope stage (Hitachi S-570 SEM, Hitachi Ltd., Tokyo, Japan). The samples were viewed at 10 kV accelerating voltage. Several representative images were collected at different magnifications from various parts of the specimens.

Results and Discussion

Effect of Aging and ISPs on the Thermal Properties of Frozen Hydrated Gluten. Typical DSC curves for frozen gluten have been published before and include two thermal events, with the minor peak being followed immediately by the major one in the increasing temperature profile of a standard thermogram (Figure 1 and refs 7 and 10). It was proposed initially that the low-temperature tail of the DSC curve is an enthalpic relaxation that accompanies the devitrification of the partially frozen system transversing the glass transition temperature (T_g').[7] An alternative approach argues that hydrated gluten forms nanocapillaries capable of entrapping water, thus introducing an extra dimension to the phase behavior of the solvent. The latter is supported by deconvoluted MDSC spectra

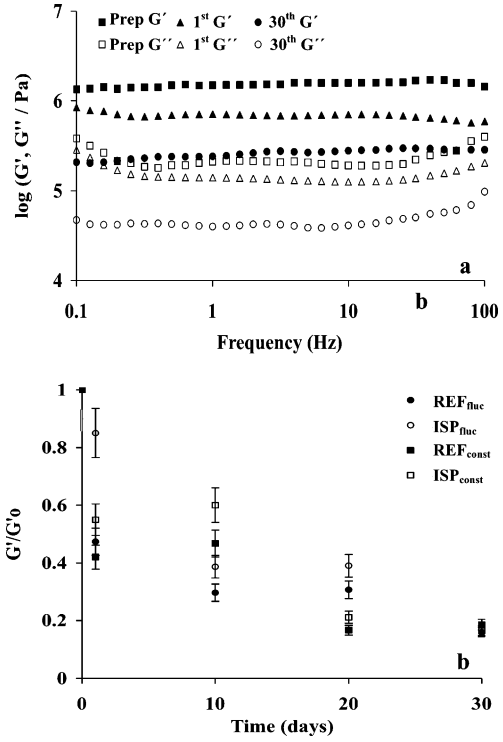

Figure 4. (a) Frequency sweeps of G' and G'' for hydrated gluten (40% w/w) that was aged at −13 °C for the number of days indicated (measurements were obtained at 20 °C and 0.5% strain) and (b) normalized values of storage modulus on shear (G') as a function of aging for the ISP and REF samples, with the storage modulus at the day of preparation being denoted as G'_0 (frequency of 1 Hz). Error bars signify one standard deviation.

of the total heat flow, which demonstrates that the minor peak appears only in the nonreversing component, hence suggesting that the peak is a first-order transition.[10] Fundamental rationalization of this process is forthcoming via the Defay−Prigogine theory of capillary-confined liquids, which takes into account the effect of curvature on the interfaces and demonstrates that the entrapped liquid has a lower melting point than its counterpart in the bulk.[19] In Figure 1, melting of capillary ice gives rise to the minor thermal event, whereas the major endothermic peak is assigned to the melting of bulk ice.

It follows that the morphology of the frozen gluten network deteriorates upon aging by two distinct mechanisms (i.e., ice formation/recrystallization in the capillary and the bulk). The relative contribution of the two processes to the loss of network functionality can be assessed by the advancement of the minor peak to higher temperatures during aging. This is demarcated as the difference ΔT between the two peaks in Figure 1, and according to the Defay−Prigogine theory, the smaller the value of ΔT, the larger the pore radius causing increasing damage in the three-dimensional gluten structure. To a first approximation, the trend in pore radius size can be obtained using the empirical equation of Landry, which has been developed for controlled pore glass samples with a cylindrical pore shape[20]

$$\Delta T = -\frac{A}{r-\delta} + B \qquad (1)$$

where A and B are parameters from least-squares regression fits of the data, r is the pore radius size of the capillary tube in nanometers, δ is the thin layer of thickness of non-freezable liquid adjacent to the pore wall, and ΔT stands for the difference between $\text{peak}_{\text{minor}}$ and $\text{peak}_{\text{major}}$ at maximum heat flow. The

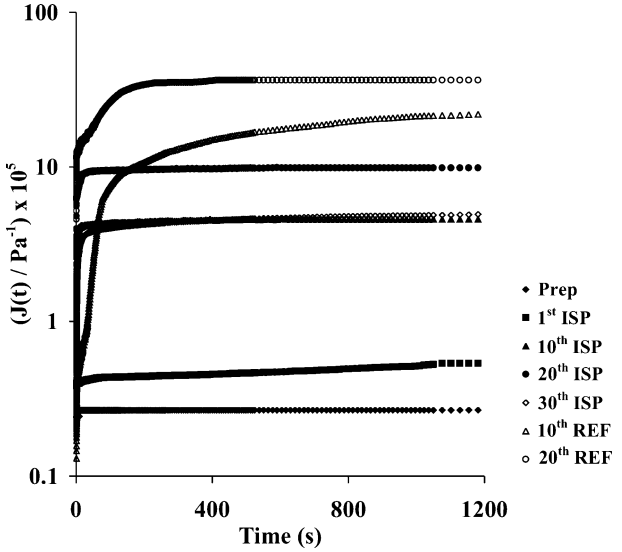

Figure 5. Creep curves of hydrated gluten (40% w/w) with (0.1% w/v) and without ISPs for samples aged at −13 °C for 30 days (measurements were taken at 20 °C; instantaneous stress was 80 Pa).

negative ΔT values reflect the observation that the pore transition temperatures are lower than those in the bulk. After rearranging the terms of eq 1 to express the pore radius, r, as a function of ΔT, and using the values of 19.082, 0.1207, and 1.12 for A, B, and δ, respectively, one can calculate the pore radius size from calorimetric data.

Table 2 summarizes a multi-dimensional matrix of changes in the enthalpy of molecular events during 30 days of aging with or without ISPs and at constant or fluctuating temperatures. In general, a maximum value is reached in the enthalpy of ice melting as a function of aging. In the absence of ISPs, similar ΔH results were obtained for model and industrial preparations of frozen hydrated gluten.[7,21] The increase in ΔH with aging is the outcome of cryodehydration of gluten leading to additional ice formation.[8,22] On the other hand, the eventual decrease in enthalpy with prolonged aging is more difficult to rationalize and may be attributed to ice recrystallization phenomena in parallel with the deterioration of the gluten matrix that results in changes in the interaction dynamics between protein and water molecules.

The present investigation builds on the previous work by introducing ISPs in the frozen hydrated gluten system. A typical gluten−ISP thermogram is depicted in Figure 1, and results are summarized in Table 2. Inclusion of the latter regardless of the experimental mode decreases consistently, albeit marginally, the enthalpy of ice melting. Ice structuring proteins were primarily effective in controlling the pore radius in mixtures exposed to constant temperature throughout. Aging increased considerably the size of the pore radius and the volume expansion of water confined in nanocapillaries for all samples, with ISPs being able to control somewhat this capillary recrystallization. Besides the data in Table 2, this is also shown in Figure 1, where the low-temperature tail of the DSC curve shifts to the left in the presence of ISPs, an outcome that should slow down structural deterioration of the gluten network.

Water Mobility Aspects of the Gluten−ISP System. This section continues the study of the micromolecular characteristics of frozen gluten with or without added ISP using time domain-^{1}H NMR. Figure 2 reproduces typical T_2 relaxation distributions of the materials recorded over 30 days of aging. They were obtained via the integral of eq 2, which is a positive sum of the

Table 3. Effect of Aging at Subzero Temperatures and ISPs on the Creep Compliance Parameters of Hydrated Gluten (40% w/w)

time (days)	J_o ($\times 10^{-5}$ 1/Pa)	J ($\times 10^{-5}$ 1/Pa)	J_o^e ($\times 10^{-5}$ 1/Pa)	η_o ($\times 10^5$ Pa s)	r^2
		REF constant			
prep	5.4	15	20.4	125	0.956
1	7.1	14	21.1	100	0.824
10	9.9	1684	1693	50	0.989
20	832	2148	3016	25	0.972
30	24	17	41	50	0.971
		ISP constant			
prep	18	2.9	20.9	50	0.718
1	32	10	42	25	0.881
10	209	138	347	11	0.891
20	480	295	775	10	0.899
30	74	262	336	25	0.947
		REF fluctuating			
prep	4.5	6.9	11.4	125	0.985
1	9.2	5.7	14.9	100	0.974
10	106	219	325	20	0.934
20	344	420	764	12.5	0.885
30	26	256	282	110	0.997
		ISP fluctuating			
prep	8.5	3.2	11.7	50	0.900
1	32	5	37	25	0.778
10	44	250	294	16	0.963
20	58	263	321	11	0.995
30	27	44	71	25	0.916

exponential decays of the signal amplitude, M, as a function of time, t, following the first pulse:[23]

$$M(t) = \int_0^\infty F(T) \exp\left(-\frac{t}{T}\right) dT \qquad (2)$$

where $F(T)$ is the number density of protons with relaxation time T. Eq 2 is effectively a Laplace transform and can be solved for $F(T)$ using a constrained regularization method for data inversion.[24,25] The reported distributions (Figure 2) are averaged distributions after Laplace inversion of the data.

Three main distributions can be distinguished in Figure 2 having T_2 ranges of 2−10, 20−70, and 120−270 ms. Experimental error of the mean of the distributions was approximately 2% for all samples studied. Esselink et al.[8] observed a T_2 relaxation time distribution at about 10 ms and assigned it to small amounts of starch present in the gluten fraction, although such cross-contamination was not evident. An explanation based on binding modes and dynamics of the starch−water system is rather unlikely presently since our system contains negligible amounts of starch, which is untraceable in the micrographs obtained in this investigation. Distribution 1 in Figure 2 probably originates from protons that are strongly associated with the gluten matrix (amino acids and low-mobility water molecules), thus being able to exchange energy and relax rapidly.

The population of short T_2 values is sensitive to aging, as is demonstrated by the variation in amplitude and width of the peak with an increasing time scale of observation (0−30 days). It should be noted that the distribution did not exhibit a clear trend during aging but showed a tendency to move to lower relaxation times with increasing storage time, an outcome that may reflect enhanced associations between the proteinaceous macromolecules (Figure 2a,b). In that case, protons would be strongly interacting and exchanging energy rapidly, thus decaying to equilibrium with accelerated rates.

As illustrated in Figure 2, the second and third distributions remain largely at their original state during aging. Similarly, addition of ice structuring proteins preserves the variability at the shortest T_2 values and leaves unaffected the last two populations at higher T_2 values (Figure 2b). The relaxation profile of the gluten−ISP mixture indicates that changes in proton mobility in the multi-layer of gluten−water interactions (to use a simple description of molecular distributions) are rather subtle. At very long T_2 values, population 3 should originate from weak associations of water from the bulk phase with gluten. The relative constancy of the final population with frozen storage suggests that the gradual recrystallization of the capillary confined water identified with distribution 1 is a critical determinant of the morphology of the gluten matrix during aging. These changes in physical state may be probed with mechanical measurements.

Macromolecular Considerations on the Phase Behavior in Gluten−ISP Mixtures. In this section, we develop the micromolecular understanding pursued with calorimetry and NMR by addressing macromolecular processes underlying the mechanical behavior of the thawed material. The design of meaningful experiments using the technique of small-deformation dynamic oscillation on shear requires recording measurements within the linear viscoelastic region (LVR) of the material. Figure 3 shows changes in the viscoelastic functions of G' and G'' for freshly prepared hydrated gluten with an increasing amplitude of oscillation at 20 °C. The limit of the LVR region was considered arbitrarily as the point where readings decrease in excess of 3% from equilibrium (inset in Figure 3). This was found to be 0.007 (0.7%), and hence, the operational strain of 0.005 (0.5%) lies comfortably within the linear viscoelastic region of the material. Estimates of the limit of linearity for the gluten network have been reported by Uthayakumaran et al.[26] (3%) and Lefebvre et al.[6] (10%). It must be noted that the limit depends on the amount of water in the system, the mechanical history of gluten, the amount of residual starch, and the protein composition of the gluten matrix (i.e., the ratio of glutenin/gliadin, etc). Therefore, the wide range of strains for

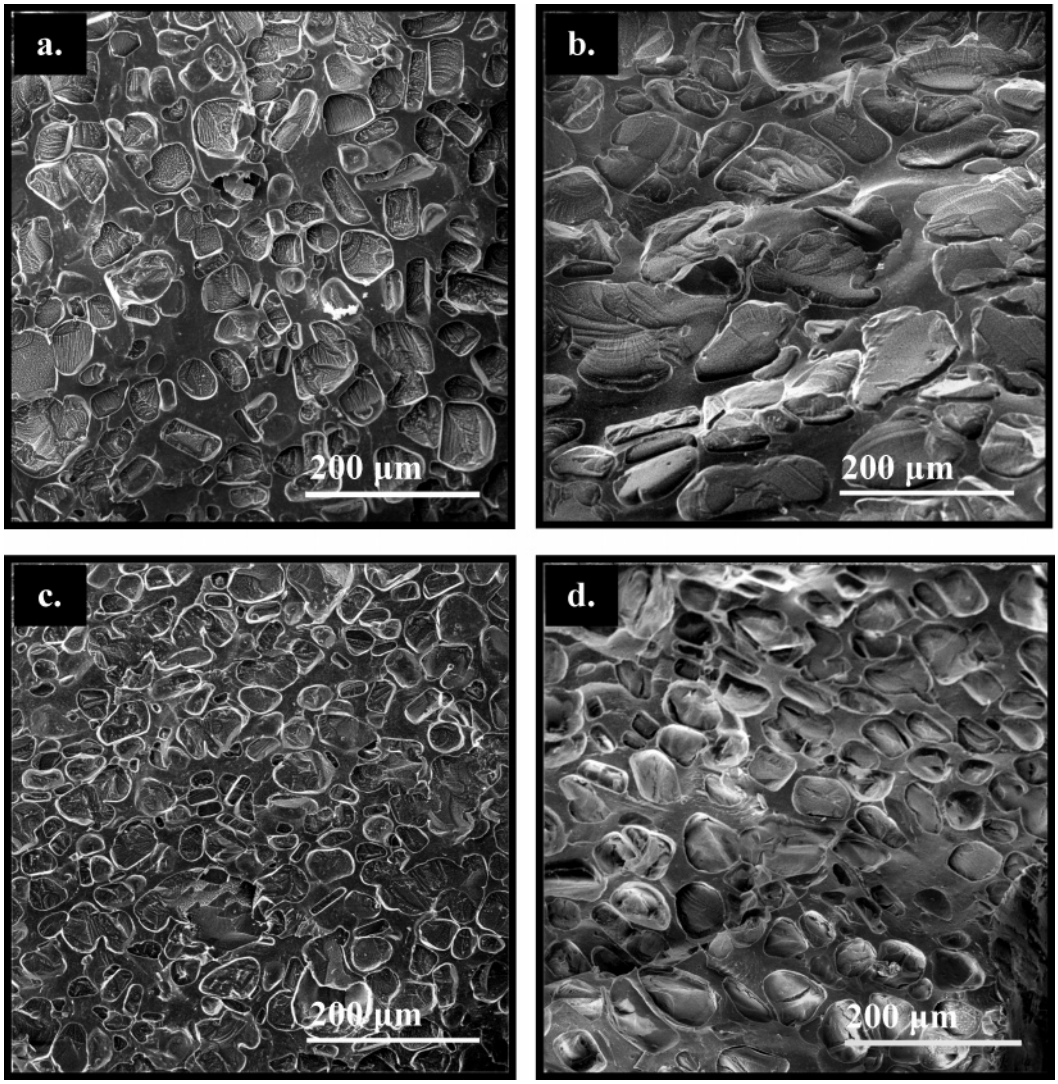

Figure 6. cryo-SEM images of the microstructure of frozen hydrated gluten (40% w/w) aged under fluctuating temperature conditions: (a) REF after 1 day of aging, (b) REF after 30 days of aging, (c) ISP after 1 day of aging, and (d) ISP after 30 days of aging.

the limit of linearity that is reported can be attributed to sample and sample preparation differences.

As illustrated in Figure 4a, the frequency dependence of storage and loss modulus for 40% gluten resembles the mechanical spectra obtained for biopolymer gels. Within the time scale of experimental measurement (0.1−100 Hz), a solid-like response predominates over the viscous flow with little frequency dependence in either. Increasing duration of frozen storage results in a considerable loss of network functionality due to the disruption of the proteinaceous junction zones by ice. At early stages of aging, a loss of mechanical strength is mainly due to ice formation, and this effect should be supplanted by ice recrystallization at longer periods of isothermal storage at −13 °C. These results are in qualitative agreement with evidence from calorimetry, which showed increasing capillary porosity in the gluten network with aging (Table 2).

To grasp the course of mechanical loss upon aging, data of storage modulus recorded at 1 Hz have been normalized with the corresponding value at the day of preparation (G'_0) and are plotted in Figure 4b. Clearly, there is a dramatic loss of elasticity, about 50% within the first day and 80% upon completion of the storage cycle. In general, inclusion of ice structuring proteins in the system results in a noticeable deceleration of the adverse effect of ice crystals on the functionality of the gluten matrix.

Further information about changes in the internal structure of the gluten−ISP system at measuring times longer that 10 s (0.1 Hz) can be obtained with creep testing. The continuous pattern of flow that emerges following application of the instantaneous stress can be described with adequate precision by a discrete retardation spectrum.[27,28] To facilitate comparisons of long time rearrangements in the gluten matrix with and without ISPs, a discrete exponential model of the experimental compliance, $J(t)$, was considered to be adequate:[29,30]

$$J(t) = J_0 + J_1(1 - e^{-t/\lambda}) + \frac{t}{\eta} \qquad (3)$$

where, J_0 is the instantaneous compliance, J_1 is the retarded compliance, λ is the retardation time of the Kelvin component, and η is the steady-shear viscosity. On the basis of eq 3, the steady-state compliance (J_0^e) is given by the sum of J_0 and J_1. Nonlinear regression was used to fit the experimental data to this mathematical expression constraining parameters J_0, J_1, and λ to be greater than zero. Linear regression of the terminal region of the creep curve was used to calculate the steady-shear viscosity, with the slope of the regression line being the inverse of the steady-shear viscosity.

Figure 5 reproduces typical creep measurements for thawed gluten with or without added ISPs, and curves are plotted in a

semilogarithmic form to facilitate a clear depiction and subsequent comparisons. In addition, Table 3 summarizes the outcome of treating the pseudo-equilibrium form of representative creep curves using eq 3 and the quality of agreement between experimental data and predictions of this model. The parametrization of compliance (J_0^e, J_0, and J_1) yields increasing values in the first 20 days of frozen storage, an outcome that indicates structural deterioration of the gluten network. In parallel, values of steady-shear viscosity have been decreasing further, confirming these changes in macromolecular morphology. As shown in Figure 5, introduction of ISPs to the system resulted in a considerable decrease of the corresponding compliance values, thus preserving the elastic component of the gluten matrix. It is noteworthy that whereas initial ice formation and recrystallization affect adversely the structural properties of hydrated gluten, longer timescales of aging (i.e., beyond day 20 in this investigation) see a turnaround in the molecular indicators describing such a structure (e.g., Table 3 and Figure 5). As freezing proceeds, an increasingly gluten-rich phase is formed that enhances the interactions between polymeric segments. Alteration of the overall composition of β-sheet and β-turn conformations because of this low-temperature cryo-denaturation cannot be ruled out as an additional cause of the observed reversal in viscoelasticity.[3] It appears, therefore, that when the concentration of the unfreezable gluten matrix is sufficiently increased, following equilibration of the ice phase, subsequent macromolecular rearrangements result in partial recovery of the protein network. Finally, rheological measurements of gluten with added gliadin subfractions have shown that ω-gliadins do not interact as much with gluten as α-, β-, or γ-gliadins.[31] This suggests that the rheological as well as the rest of the properties (thermal, water dynamics) are likely to depend on the amount and type of gliadins in gluten. In conclusion, undertaking work on creep testing, and in combination with the shorter timescales of dynamic oscillation on shear, clearly demonstrates the utility of ice structuring proteins as potent agents in preservation of the functional quality of frozen gluten.

Tangible Evidence of the Effect of ISPs on Frozen Hydrated Gluten upon Aging. To assist in the rationalization of the previous findings, we employed cryo-scanning electron microscopy, which is a technique capable of providing tangible evidence of the transformation in the three-dimensional morphology of hydrated gluten during frozen storage. Figure 6 a−d reproduces images of the protein network in the presence or absence of ISPs taken for systems subjected to fluctuating temperature conditions. The dominant features of these images are the continuous gluten phase surrounding irregular round-etched domains occupied by ice crystals prior to sublimation.

Microstructural characteristics vary considerably with aging, and ice crystals in the reference sample appear to be significantly larger on the 30th day, owing to recrystallization. The process of cryo-shrinkage of the gluten network decreases the interstitial regions of the protein that separate adjacent ice crystals leading to mechanical damage in the microstructure. Addition of ice structuring proteins did not bring about convincing qualitative differences in the ice−gluten composite at the first day of aging. In contrast, ISPs appear to have considerable impact at longer periods of storage by inhibiting recrystallization and thus controlling the ultimate size of the ice crystals. The morphological observations of the present section further support the outcome of physicochemical analysis on the relationship between ISP functionality and time-driven ice growth in hydrated gluten.

Conclusion

Molecular understanding of the phase behavior and structural properties of the frozen gluten network as a function of aging and in the presence of ice structuring proteins was pursued in view of the considerable industrial applications pertaining to these systems. Thermal, mechanical, and NMR analysis as well as electron microscopy unveil an increasing degree of functional loss in the gluten matrix within the first 20 days of storage. Experimentation and first principles modeling allowed deconvolution of this outcome into the molecular processes of ice formation and recrystallization. Incorporation of ice structuring proteins was found to decelerate structural changes in the gluten−ice composite during the recrystallization stage. Furthermore, storage at a constant temperature just below the onset of ice melting had a more detrimental effect on the mechanical features of the gluten network as compared with aging under fluctuating temperature conditions. Thus, since pinpointing T_g in frozen hydrated gluten is ambiguous, consideration of the melting point of ice may provide an alternative approach of quality control in these systems.

Acknowledgment. The authors thank the Greek State Scholarships Foundation and the Natural Sciences and Engineering Research Council of Canada for financial support and Dr. S. Smith for technical assistance and fruitful discussions regarding the cryo-SEM part of the study.

References and Notes

(1) Carceller, J. L.; Aussenac, T. *J. Cereal Sci.* **2001**, *33*, 131.
(2) Wahlund, K. G.; Gustavsson, M.; MacRitchie, F.; Nylander, T.; Wannerberger, L. *J. Cereal Sci.* **1996**, *23*, 113.
(3) Belton, P. S. *J. Cereal Sci.* **1999**, *29*, 103.
(4) MacRitchie, F.; Lafiandra, D. Structure−function relationships of wheat proteins. In *Food Proteins and Their Applications*; Damondaran, S., Paraf, A., Eds.; Marcel Dekker Inc.: New York, 1997; pp 293.
(5) Don, C.; Lichtendonk, W.; Plijter, J. J.; Hamer, R. J. *J. Cereal Sci.* **2003**, *37*, 1.
(6) Lefebvre, J.; Pruska-Kedzior, A.; Kedzior, Z.; Lavenant, L. *J. Cereal Sci.* **2003**, *38*, 257.
(7) Bot, A. *Cereal Chem.* **2003**, *80*, 366.
(8) Esselink, E. F. J.; van Aalst, H.; Maliepaard, M.; van Duynhoven, J. P. M. *Cereal Chem.* **2003**, *80*, 396.
(9) Nicolas, Y.; Smit, R. J. M.; van Aalst, H.; Esselink, F. J.; Weegels, P. L.; Agterof, W. G. M. *Cereal Chem.* **2003**, *80*, 371.
(10) Kontogiorgos, V.; Goff, H. D. *Food Biophys.* **2006**, *1*, 202.
(11) Clarke, C. L.; Buckley, S. L.; Lindner, N. *Cryo-Lett.* **2002**, *23*, 89.
(12) Atici, O.; Nalbantoglu, B. *Phytochemistry* **2003**, *64*, 1187.
(13) Griffith, M.; Ewart, K. V. *Biotechnol. Adv.* **1995**, *13*, 375.
(14) Yeh, Y.; Feeney, R. E. *Chem. Rev.* **1996**, *96*, 601.
(15) Knight, C. A.; Wierzbicki, A. *Cryst. Growth Des.* **2001**, *1*, 439.
(16) Wilson, P. W. *Cryo-Lett.* **1993**, *14*, 31.
(17) Regand, A.; Goff, H. D. *J. Food Sci.* **2005**, *70*, 552.
(18) Kontogiorgos, V.; Regand, A.; Yada, R. Y.; Goff, H. D. *J. Food Biochem.* **2007**, in press.
(19) Defay, R.; Prigogine, I. *Surface Tension and Adsorption*; Longmans: London, 1966.
(20) Landry, M. R. *Thermochim. Acta* **2005**, *433*, 27.
(21) Lu, W.; Grant, L. A. *Cereal Chem.* **1999**, *76*, 656.
(22) Berglund, P. T.; Shelton, D. R.; Freeman, T. P. *Cereal Chem.* **1991**, *68*, 105.
(23) Parker, R. L.; Song, Y. Q. *J. Magn. Reson.* **2005**, *174*, 314.
(24) Provencher, S. W. *Comput. Phys. Commun.* **1982**, *27*, 213.
(25) Provencher, S. W. *Comput. Phys. Commun.* **1982**, *27*, 229.
(26) Uthayakumaran, S.; Newberry, M.; Phan-Thien, N.; Tanner, R. *Rheol. Acta* **2002**, *41*, 162.
(27) Kaschta, J.; Schwarzl, F. R. *Rheol. Acta* **1994**, *33*, 517.
(28) Kaschta, J.; Schwarzl, F. R. *Rheol. Acta* **1994**, *33*, 530.
(29) Honerkamp, J. *Rheol. Acta* **1989**, *28*, 363.
(30) Istratov, A.; Vyvenko, O. F. *Rev. Sci. Instrum.* **1999**, *70*, 1233.
(31) Khatkar, B. S.; Fido, R. J.; Tatham, A. S.; Schofield, J. D. *J. Cereal Sci.* **2002**, *35*, 307.

BM0610471